Glycoconjugate Journal 19, 43–52, 2002

An NMR study of *O*-glycosylation induced structural changes in the α-helix of calcitonin

Mizuka Tagashira[1], Hideki Iijima[1] and Kazunori Toma[2*]

[1] *Analytical Research Laboratory, Asahi Kasei Corporation, Fuji, Shizuoka 416-8501, Japan,* [2] *The Noguchi Institute, Itabashi, Tokyo 173-0003, Japan*

We previously reported that two out of seven artificially *O*-glycosylated calcitonin derivatives had an altered peptide backbone conformation as indicated by decreased helical contents, determined by CD measurement. In the present study, two of those derivatives, in which a GalNAc residue is attached to Thr6 or Thr21 of calcitonin, were analyzed by NMR in order to determine the structural changes induced by the *O*-glycosylation in more detail. Deviations in the chemical shifts suggest that the structural change is not global but only a local one and is located in the vicinity of each *O*-glycosylation site. The intensities of the NOE cross peaks, an indicator of α-helical structure, also were decreased around the *O*-glycosylation site. The hydrogen/deuterium exchange rates of the main chain amide protons increased at the N- or C-terminal portion of the α-helix corresponding to the respective *O*-glycosylation site and explains the results of the CD experiments. The inter-residual NOE cross peaks between the carbohydrate and the peptide portions, other than the *O*-glycosylated amino acid residue, showed that local structural contacts extended three or two residue distance for Thr6- or Thr21-glycosylated derivative, respectively. Thus, we conclude that the *O*-glycosylation induced a change in the local structure and that this structural perturbation modulated the original α-helical structure of calcitonin, resulting in the apparent decrease in the helical content deduced from CD spectra.

Keywords: **calcitonin, glycosylation, glycopeptide, structural changes, NMR analysis**

Introduction

The carbohydrate moieties of glycoproteins and glycopeptides are believed to have important roles in their biological activity [1,2]. Among these, the structural effect on a peptide backbone represents a major function, since carbohydrate structures are of significant size compared to the protein or peptide portions [3,4]. However, the issue of how glycosylation affects protein or peptide structure is unclear. Some investigators have reported that a carbohydrate moiety aids in the formation of a secondary structure of a peptide backbone, especially the β-turn [5–7], or stabilizes the peptide backbone conformation [8,9]. In some cases no structural change is evident [10,11], and in one extreme case the original α-helical structure was found to be broken [12].

During our systematic studies on the three-dimensional structure and biological activity of artificially *N*- and *O*-glycosylated calcitonin (CT) derivatives [13–17], we found that the structural effect of glycosylation was site-specific.

CT is a peptide hormone with hypocalcemic activity, and is comprised of 32 amino acid residues [18] (see Figure 1). The natural form of CT is not glycosylated, and CT assumes a three-dimensional structure in hydrophobic environments [19–21]. Relationships between the three-dimensional structure of CT, induced by a hydrophobic environment, and its biological activity have been discussed, because CT is believed to assume an α-helical structure by interacting with a membrane prior to its binding to its receptor on the membrane [22].

Based on CD data, CT assumes an ca. 60% helical content in an aqueous 40% solution of trifluoroethanol (TFE) [14]. The CD spectra indicate that artificial *N*-glycosylation, i.e., GlcNAc attachment or successive transfer of natural oligosaccharides to the GlcNAc by endo-glycosidases, at Asn3, Gln14, Gln20 or Asp26 (in the last case, Asp was replaced by Asn) of CT had no effect on the α-helical structure of the peptide backbone [13–15]. Among the seven *O*-glycosylated derivatives at Ser2, Ser5, Thr6, Ser13, Thr21, Thr25 or Thr31, only [Thr(GalNAc)^{6}]-CT (CT6-GalNAc) and [Thr(GalNAc)^{21}]-CT (CT21-GalNAc) were found to have a helical content that was decreased by ca. 10% compared with CT in aqueous 40% TFE [16]. Thus, the structural effect of glycosylation appears to be dependent on the glycosylation site [17].

In our previous report, we proposed that the attachment of GalNAc residue made the glycosylated amino acid residue a

*To whom correspondence should be addressed: Kazunori Toma. Tel. & Fax: +81-3-5944-3216; E-mail: toma@noguchi.or.jp

stronger helix breaker [16], using an analogy to secondary structure propensities of amino acids, although the precise reasons for this are unclear. To better understand the nature of this structural change, the NMR spectra of CT6-GalNAc and CT21-GalNAc in the same 40% TFE aqueous solution condition as was used to obtained the CD spectra were examined.

Materials and methods

The eel CT amino acid sequence was employed, and the preparation of CT6-GalNAc and CT21-GalNAc has been reported in a previous paper [16]. The samples were dissolved in a 40% aqueous solution of TFE (TFE-d_2/H_2O/D_2O = 4/5/1), at a concentration of ca. 5 mM. NMR spectra were obtained with a JEOL JNMA-500 spectrometer using an NH3X/FG probe supplied by NALORAC Corp. A series of two-dimensional NMR experiments, DQF-COSY, TOCSY and NOESY, were performed at 10°C in the phase-sensitive mode. Water signals were suppressed using a 2-sec pre-saturation pulse during the recycle delay. The NOESY spectra were recorded for several mixing times: 80, 150 and 200 ms. The TOCSY spectra were recorded using an 80-ms mixing time for the magnetization transfer. Data processing was performed using the FELIX software (Molecular Simulations, Inc.). Assignments of the proton signals were mainly made using the sequence-specific assignment method reported by Wüthrich [23]. In order to overcome difficulties in making the assignments due to signal overlapping, NOESY experiments were also performed on a Varian INOVA 750. The exchange of amide protons with deuterium was examined by NOESY measurements with a 200-ms mixing time at 10°C. Samples used in the hydrogen/deuterium (H/D) exchange experiments were prepared in a deuterium solution of 40% TFE (TFE-d_2/D_2O = 4/6), at the same concentration as was used in the other experiments. One measurement required 5 hours, and the measurement was consecutively repeated 5 times, providing time-dependent spectra for 5-hour intervals. The intensities of the signals were obtained from the spectra, and the exchange rate constants were calculated by fitting the data to the exponential decay function.

Results

The amino acid sequence of eel CT and the seven *O*-glycosylation sites are shown in Figure 1. A single GalNAc residue is attached to the Thr or Ser side chain hydroxyl

Figure 1. The amino acid sequence of eel CT in single letter amino acid codes. Cys1 and Cys7 form a disulfide bond. The artificially *O*-glycosylated sites in a previous study [16] are indicated by arrows. Bold arrows show the two derivatives, CT6-GalNAc and CT21-GalNAc, analyzed in this study.

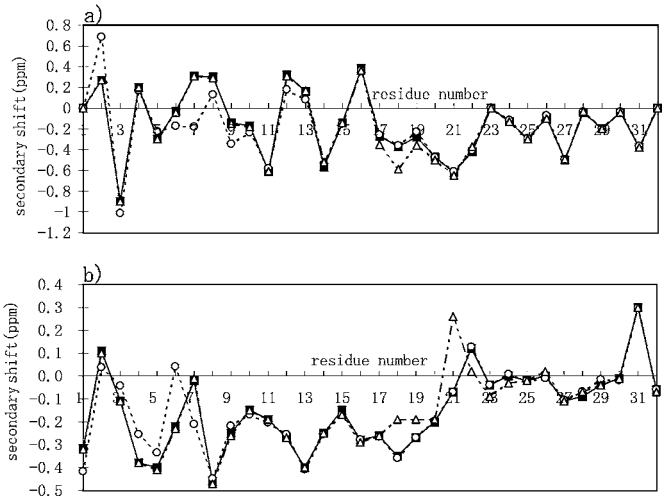

Figure 2. Secondary shift differences in NH (a) and CαH (b) proton resonances: CT (■; solid line), CT6-GalNAc (◯; broken line) and CT21-GalNAc (△; dots and dashes). Secondary shifts are the differences in the chemical shifts from those in a random coil structure [23]. An α-helical structure can be recognized by successive negative secondary shifts in CαH.

group of CT in the α-anomeric configuration. CT6-GalNAc and CT21-GalNAc in which structural changes had been previously detected by CD spectra were analyzed by NMR, and the magnitude of the structural changes was determined using CT as a reference.

The 2D-NMR spectra allowed the assignment of the majority of the signals. Figure 2 shows the NH and CαH chemical shifts for CT, CT6-GalNAc and CT21-GalNAc as secondary shifts, which are the differences in the chemical shifts from those in a random coil structure [23]. Although Ogawa et al. previously reported on the chemical shifts of eel CT [24], our data [14] are used for comparison, because there were slight differences in the experimental conditions between our experiments and those used by Ogawa et al.

The NH chemical shifts of CT6-GalNAc in Figure 2a deviate from those of CT at residues 2 to 10, 12 and 13. The CαH chemical shifts shown in Figure 2b also show differences in residues 1 to 11. For CT21-GalNAc, the NH and CαH chemical shifts show deviations from CT at residues 18 to 19 and at 18 to 24, respectively. Such wide-range deviations in the NMR chemical shifts serve to indicate that the three-dimensional structures of CT6-GalNAc and CT21-GalNAc are different from CT, whereas the other glycosylated derivatives were structurally similar. The chemical shifts for a sample in which GlcNAc was attached to Asn3 deviated to a much lesser extent from CT itself [13]. Such differences can be atributed to the change in magnetic environment due to the introduction of GalNAc, if the chemical shift deviations were restricted to residues in the close vicinity of the GalNAc attachment sites. The observed deviations, however, ranged over a much wider region.

A more plausible explanation for the above findings is that the chemical shift deviations are the result of a decrease in

the helical content, as observed in the CD spectrum [16]. The CαH peaks are known to shift up-field in the case of α-helical structures compared with those in random-coil structures, and α-helices can be recognized by successive negative secondary shifts in CαH [23]. In the analysis of CT, the secondary shifts showed negative values at residues 4 to 20, suggesting an α-helical structure in this portion of the molecule [14]. Although the precise position depends on the origin of CT and the experimental conditions, other NMR studies of CT also report similar α-helical structures [19,20,24]. The chemical shifts of CT6-GalNAc and CT21-GalNAc used in this study were different from CT in the vicinity of the glycosylation sites corresponding to the N- and C-terminal portions, respectively, of the α-helix. The absolute values of the secondary shift of CαH became smaller at residues 4 (-0.38 to -0.26), 5 (-0.40 to -0.34) and 6 (-0.22 to 0.04) for CT6-GalNAc, and residues 18 (-0.35 to -0.19) and 19 (-0.27 to -0.19) for CT21-GalNAc, suggesting that the α-helical structure is modulated locally, as the result of *O*-glycosylation.

Because the direct magnetic effect of the introduction of GalNAc and effects arising from structural changes induced by the attachment of GalNAc residue may be difficult to discern from only chemical shifts, we also examined changes in α-helical structure by the NOE connectivity pattern, and the results are summarized in Figure 3a and b for CT6-GalNAc and CT21-GalNAc, respectively. An NOE cross peak with an interval of 3 residues, such as $d_{\alpha\mathrm{N}}(i, i+3)$ and $d_{\alpha\beta}(i, i+3)$, indicates a typical α-helical structure, and the ith and $(i+3)$th

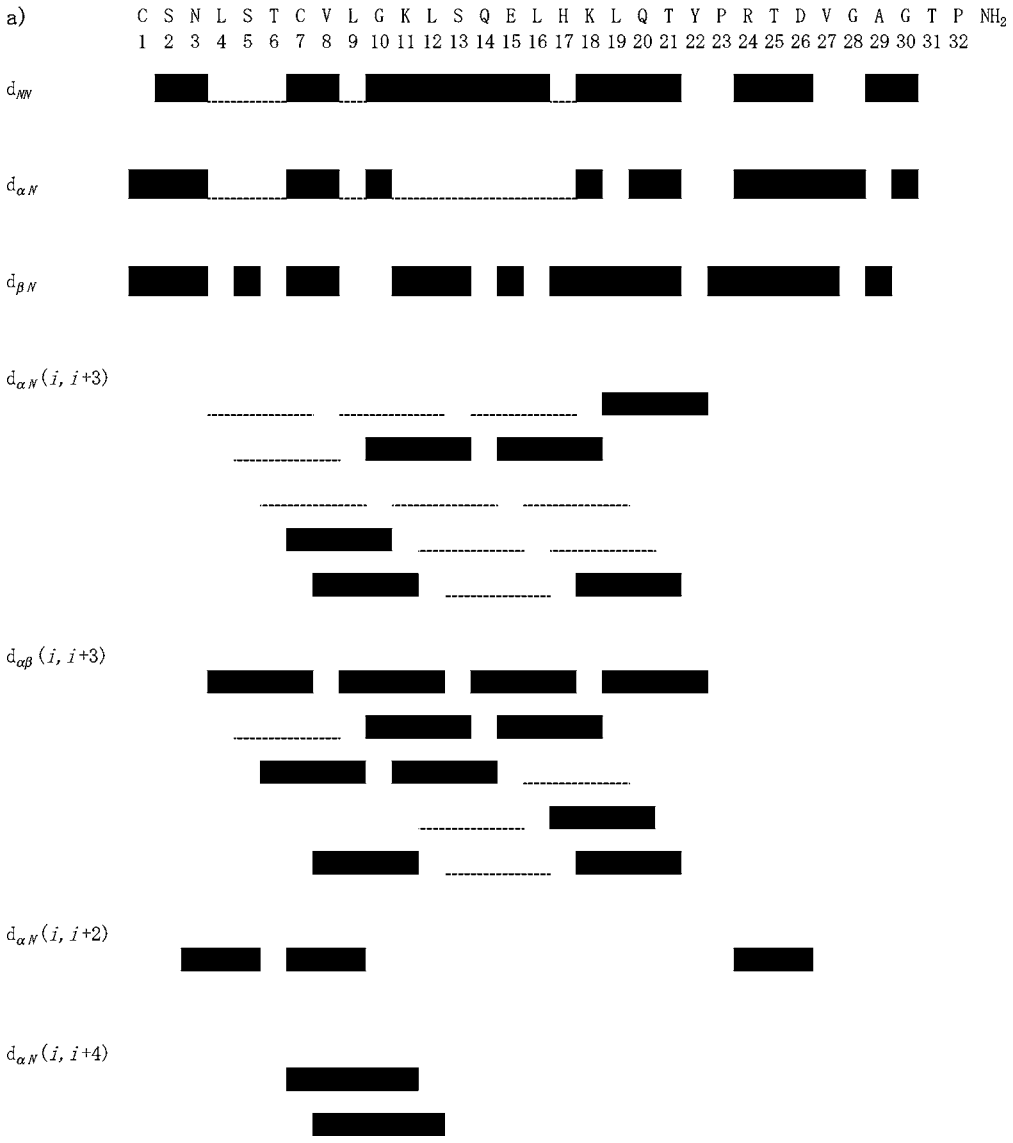

Figure 3. NOE connectivities of CT6-GalNAc (a) and CT21-GalNAc (b). The $d_{\mathrm{AB}}(i, j)$ notation follows that proposed by Wüthrich [23]. A solid band indicates that an NOE cross peak was observed between AHi and BHj protons. Dashed underlines show unidentified cross peaks due to signal overlapping. (*Continued on next page.*)

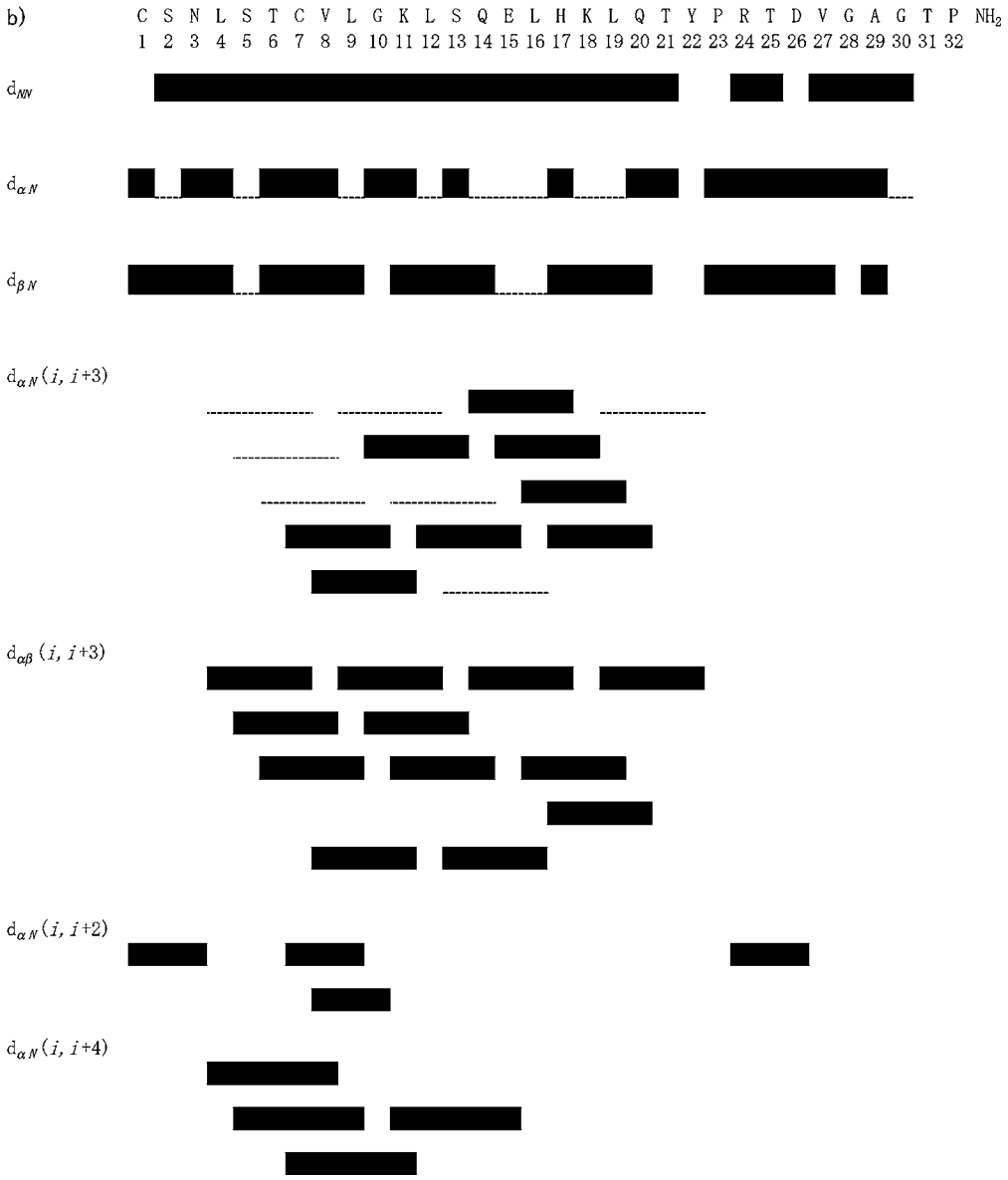

Figure 3. (*Continued*).

residues are in an α-helical configuration. Such NOE cross peaks were observed for residues 4 to 22 of CT6-GalNAc, which corresponds to the α-helical region. Unfortunately, the NOE signals of the N-terminal portion of the region was overlapped by other signals, thus making the assignments difficult. These portions are shown as dashed underlines in Figure 3. However, it was clear that the intensity of the NOE cross peak between CαH4 and CβH7 in CT6-GalNAc was reduced to half of that of CT or CT21-GalNAc, shown in Figure 4 as relative intensities to the reference CδH32 signal, providing evidence for the local modulation of the α-helix at this position. In the spectra of CT21-GalNAc, a $d_{\alpha\mathrm{N}}(i, i+3)$ cross peak for CαH18-NH21 was not observed at the C-terminal region of the α-helix, although cross peaks corresponding to CαH17-NH20 and CαH19-CβH22 were observed and CαH19-NH22 may also exist in overlapping signals. Thus, *O*-glycosylation at residue 21 also appears to disrupt the α-helical structure at this glycosylation site.

Both the chemical shift and the NOE pattern indicate that α-helical structure around each *O*-glycosylation site is perturbed, but this may not be sufficient to explain the 10% decrease in α-helical content determined by CD measurement. Therefore, another more quantitative structural analysis of the α-helical structure was performed by means of H/D exchange experiments. Although slow H/D exchanges generally indicate that exchangeable protons are shielded from the solvent environment, it would normally be expected amide protons in the α-helix would be the participants, because the main CT structure is an α-helix. In the α-helical region, amide protons that are hydrogen-bonded to carbonyl oxygen atoms that precede one

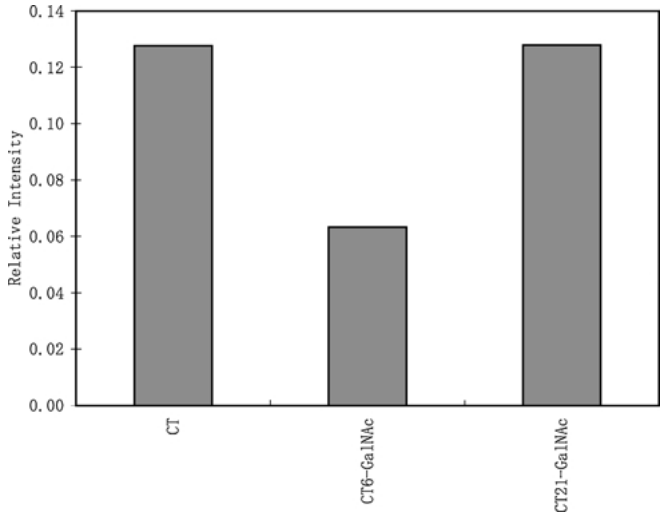

Figure 4. Relative intensities of the NOE cross peaks between CαH4 and CβH7 in CT, CT6-GalNAc and CT21-GalNAc. The signal intensity of Cδ proton of Pro32 is used as a reference.

helical pitch, i.e., 3 amide bond units, and amide protons become protected from exchange with solvent deuterium. H/D exchange can be observed by NH signal decay in D_2O using NMR. We employed the NOESY technique and measured the intensities of the cross peaks arising from the amide protons. The NH signals of CT corresponding to the α-helical region persisted for more than 10 hours in the solution. This confirms that these signals could be used as indicators of hydrogen-bonds in the α-helix. We then carried out the same measurements for CT6-GalNAc and CT21-GalNAc, and, in these cases, slow exchange NH protons were found as shown in Figure 5.

The NOESY spectra of CT showed a slow exchange of NH signal for residues 5 to 22, respectively. This region encompasses the α-helical structure, as revealed by observations of the sequential NOE pattern and the secondary shift of CαH. The slow exchange region extended toward the N-terminal loop structure, which is characterized by a disulfide bridge between Cys1 and Cys7. Because amide protons in an α-helix are hydrogen-bonded to the carbonyl group that precedes it by 3 amide bond units, the NH of residues 5 to 7, located at the N-terminal edge of the α-helix have no pairing carbonyl groups. Therefore, we presume that the N-terminal loop structure also protects those amide protons from H/D exchange. In the case of CT21-GalNAc, the region was reduced to residues 4 to 20. The hydrogen-bonds became considerably more weak at the C-terminal end of the α-helix. Unlike CT21-GalNAc, the pattern for CT6-GalNAc in Figure 5 was similar to that of CT, indicating that the slow exchange region was from residues 5 to 22. However, the NOESY signal decayed more rapidly at the N-terminal end of the α-helix.

Figure 6 compares the time-dependent changes in the NOESY signal intensity of each residue for CT, CT6-GalNAc and CT21-GalNAc. The graphs in the figure show residues where the assignment of the amide proton was possible for all three compounds. The signal intensity of the three derivatives is similar in the middle of the α-helix, such as the Leu16 amide proton, where the effect of glycosylation is negligible. It therefore appears that the time course for signal decay is the most sensitive indicator of structural changes in the α-helical region. We also calculated the H/D exchange rate constants from the data and these are summarized in Figure 7. Cases where signal assignments were difficult are not shown in this figure.

Even for CT, the H/D exchange rate was a function of position. At both the N- and C-termini of the α-helix, the rate was faster than that at the center. Among both termini, the rate was slower at the N-terminal than at the C-terminal of the α-helix, probably because of the protective effect of the N-terminal loop structure as discussed above. Therefore, the position of the structural change must be determined by comparing the rates of exchange of neighboring residues, and must also be in agreement with other data. In CT6-GalNAc, the H/D exchange was faster than in CT and CT21-GalNAc at residues 9 to 14, though they were both assigned as slow exchange amide protons in Figure 5. Among them, the exchange rates were extremely fast at residues 10 and 11, which were hydrogen-bonded to amide bond carbonyl groups that follow residues 6 and 7, corresponding to the N-terminal portion of the α-helix. Similarly, the H/D exchange rate of CT21-GalNAc increased at residues 21 and 22, and became non-slow exchange amide protons. Though it is known that helical content, as estimated from the CD spectra, is not accurate, the observed changes in the H/D exchange rates indicate about a 2- to 3-residue reduction in helical length, and roughly correspond to a 10% reduction, i.e., ca. 3 residues for a 32-amino acid peptide, in α-helical content, as determined by CD.

Other than the helical pattern, the NOESY measurements also provide information on how the carbohydrate portion interacts with the peptide portion. In Figure 8, such inter-residual NOE signals are summarized by indicating with arrows. The carbohydrate moiety interacted not only with its attached amino acid residue but also with some, more remote residues. Figure 9 shows the parts of NMR charts in which NOE cross peaks corresponding to those interactions appear. Such local interactions

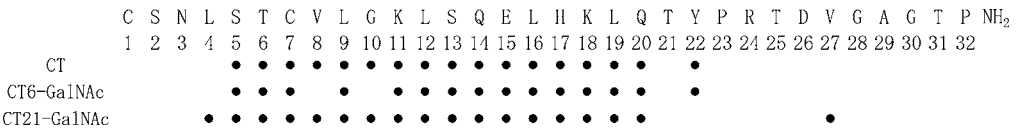

Figure 5. Slow H/D exchange amide protons of CT, CT6-GalNAc and CT21-GalNAc are indicated by closed circles. H/D exchange was measured by NH signal decay in D_2O using intensities of NOE cross peaks arising from the amide protons.

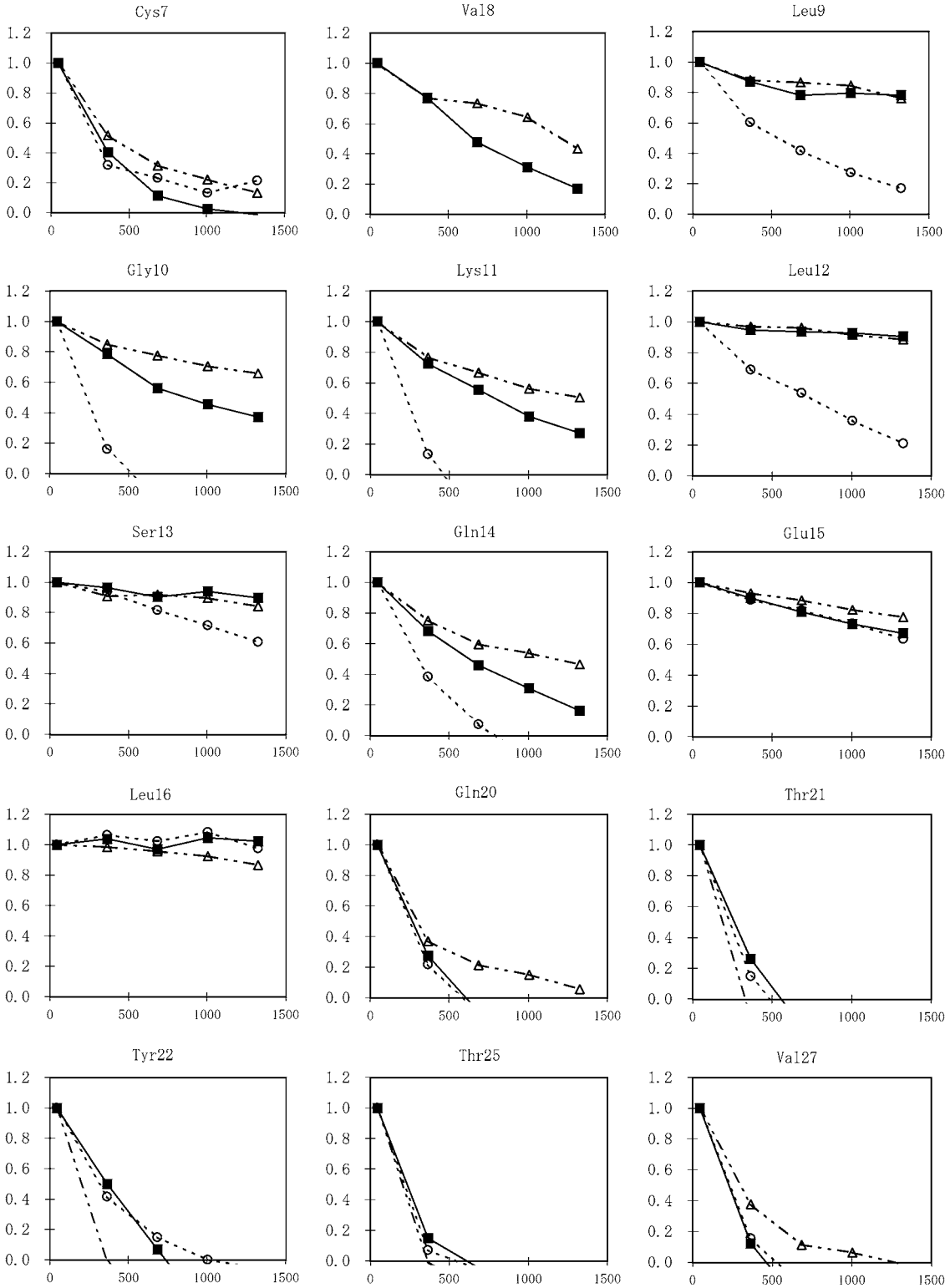

Figure 6. H/D exchange time course (in minutes) of the relative NOE cross peak intensity for each amide proton: CT (■; solid line), CT6-GalNAc (◯; broken line) and CT21-GalNAc (△; dots and dashes). Each point represents 5-hour measurement, and that was consecutively repeated 5 times, providing time-dependent chart of 5-hour intervals. Residues are shown for which the amide protons of all the compounds could be assigned.

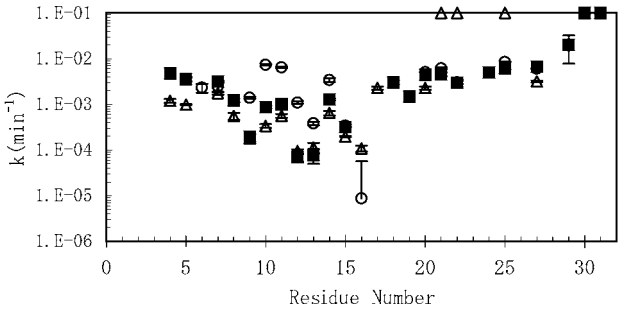

Figure 7. H/D exchange rates for each amide proton: CT (■), CT6-GalNAc (○) and CT21-GalNAc (△). The exchange rate constant is calculated by fitting the data of Figure 6 to an exponential decay function. Unassignable amide protons are not shown.

must induce local structural changes, resulting in the modulation of the α-helical structure in the vicinity of the glycosylation site.

Discussion

The data that we have reported [13–17] are unique among studies on the structural effects of glycosylation in that a series of 11 glycosylation sites on a single peptide were systematically investigated and site-specificity was clearly demonstrated. It is important to investigate the molecular mechanism of glycosylation-induced structural changes in more detail, if we are to completely understand the function of carbohydrates. CD spectra can be used to detect changes in a secondary structure, but do not specify where and how such change occur. CD experiments cannot be used to determine if such change is local around the glycosylation site or a global change in the equilibrium between helical and non-helical structures. To understand the molecular mechanism of the structural change induced by glycosylation, elaborate NMR studies are necessary.

Deviations in chemical shifts suggest that the structural change is a localized one, because the range of residues where deviations in chemical shifts are observed is cleary different between CT6-GalNAc and CT21-GalNAc. To specify the epicenter of each structural change, we examined the α-helical structure more precisely. NOE and H/D exchange experiments show that the structural change is actually confined to the region around the glycosylation site. The decrease in helical content estimated from CD spectra can also be explained from the revealed structural change, if all the data concerning hydrogen-bonds are taken into account.

It is interesting to note that a wider-range deviation in chemical shift was observed for CT6-GalNAc than for CT21-GalNAc. The wide-range chemical shift deviation at the N-terminal of CT6-GalNAc presumably arises from a change in the relative configuration of the N-terminal loop region versus the α-helix. The formation of an α-helical structure induces secondary chemical shifts [25], and the helical dipole can affect the chemical shifts of the N-terminal loop protons that are positioned in the direction of the helical dipole [26]. The loop structure must be a compact one, because it is fixed by the presence of the disulfide bond and the H/D exchange rate of amide protons is slow in this region. The structural change in CT6-GalNAc at the N-terminal of the α-helix must relocate the entire loop region relative to the α-helix. On the other hand, the C-terminal region of CT assumes a flexible random-coil structure, and nearly no effect on chemical shifts was observed after residue 24 in the case of CT21-GalNAc.

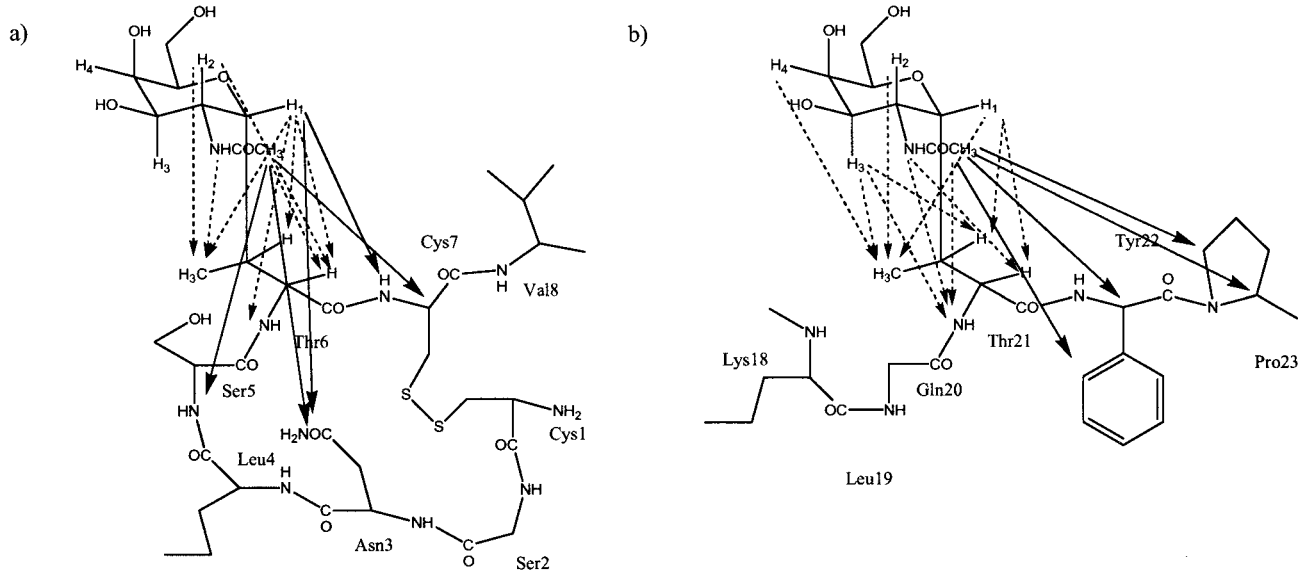

Figure 8. Inter-residual NOE connectivity observed between the carbohydrate and the peptide portions: CT6-GalNAc (a) and CT21-GalNAc (b). Solid arrows show interactions with amino acid residues other than glycosylated ones, and broken arrows indicate glycosylated ones. The former signals are shown as NMR charts in Figure 9.

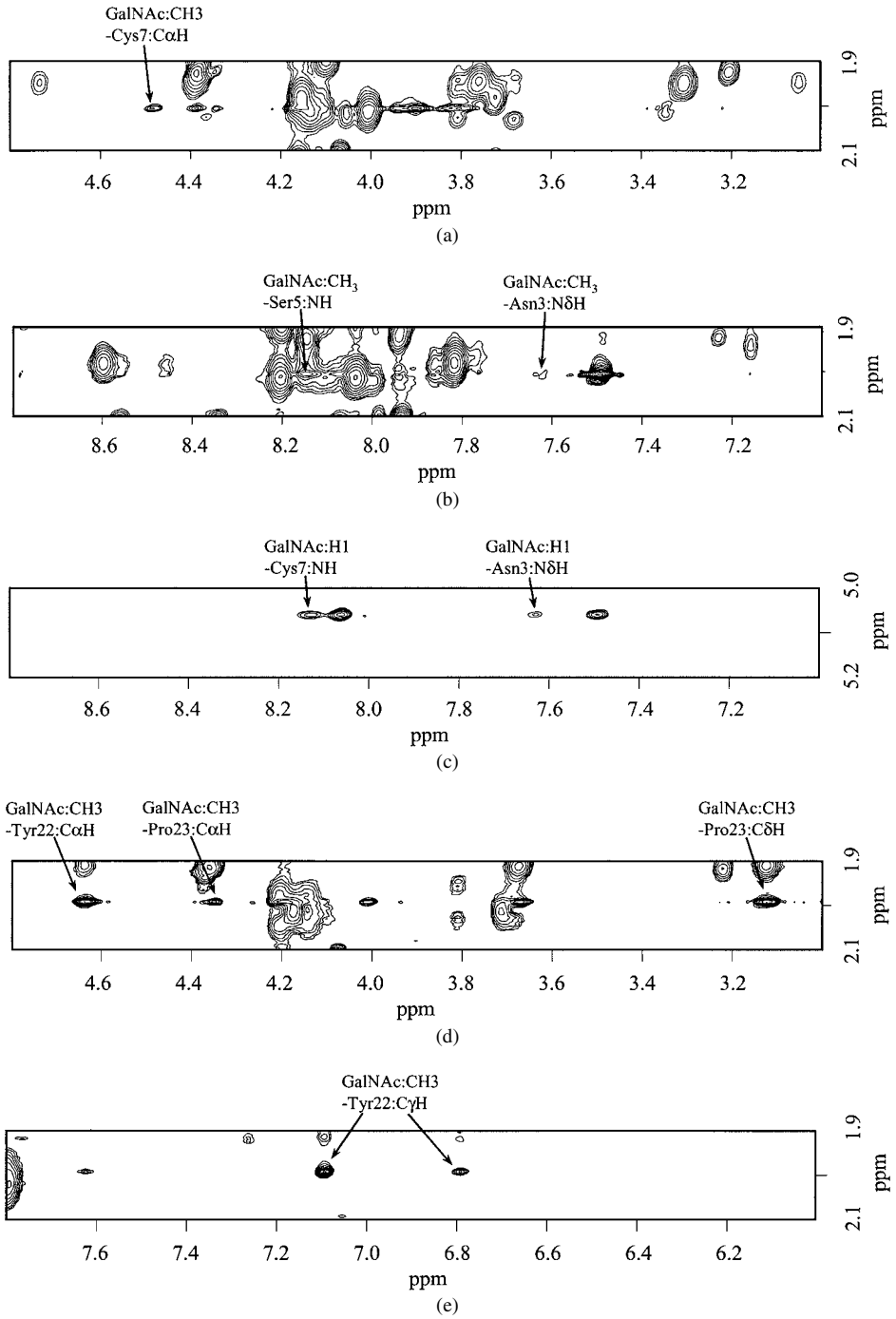

Figure 9. Inter-residual NOE cross peaks between GalNAc and amino acid residues other than the glycosylated ones. NOE cross peaks between: $COCH_3$ and CαH7 (a), $COCH_3$ and NδH3 and NH5 (b), and H1 and NδH3 and NH7 (c) of CT6-GalNAc; $COCH_3$ and CαH22, CαH23 and CδH23 (d), and $COCH_3$ and CγH22 (e) of CT21-GalNAc.

A localized structural change is also predicted from biological activity data. It is interesting to note that CT21-GalNAc retained its hypocalcemic activity in spite of a structural alteration [16]. Although this conflicting result can be explained from data on the deletion mutant, in that the C-terminal 1 pitch of the α-helix is not essential for activity [27], a structural change in CT21-GalNAc must be local to satisfy this analogy, because it is known that most of the other residues in the α-helical region are required for activity.

An interaction between the carbohydrate portion and the peptide portion other than the glycosylated amino acid residue was also found for the case of CT glycosylated at Asn3 [13]. The

GlcNAc residue attached to the side chain amide of Asn3 interacted with the side chain methyl group of Thr6, but this interaction caused the α-helical structure to be more stable. It is important to note that a fundamental change at molecular level is common for both *N*- and *O*-glycosylation in that certain local structures are formed, but the outcomes of this are different. The introduction of a carbohydrate moiety induces local contacts which may stabilize or destabilize the original conformation of a peptide backbone. Because the original peptide conformation depends on the amino acid sequence, the effect of glycosylation also depends on the amino acid sequence as well as the glycosylation site.

In conclusion, all of the NMR data presented here suggest that the *O*-glycosylation of CT at Thr6 or Thr21 led to the local structural perturbation, modulating the α-helical structure only around the respective glycosylation sites. Along with the previously reported NMR structure of *N*-glycosylated CT, we now have a more general understanding of the effect of glycosylation on overall peptide conformation.

Acknowledgments

We thank Dr. Y. Hashimoto and Mr. K. Ogawa (Asahi Kasei Corporation) for their valuable comments on the NMR studies of CT. We also thank Dr. K. Adachi (Marine Biotechnology Institute) and Ms. Y. Kobayashi (Research Center for the Industrial Utilization of Marine Organisms) for their practical help with the NMR measurements. This work was performed as a part of the Research and Development Project of Industrial Science and Technology Frontier Program supported by NEDO (New Energy and Industrial Technology Development Organization).

References

1 Varki A, Biological roles of oligosaccharides: All of the theories are correct, *Glycobiology* **3**, 97–130 (1993).
2 Lis H, Sharon N, Protein glycosylation—structural and functional aspects, *Eur J Biochem* **218**, 1–27 (1993).
3 Dwek RA, Glycobiology: Toward understanding the function of sugars, *Chem Rev* **96**, 683–720 (1996).
4 Imperiali B, Protein glycosylation: The clash of the Titans, *Acc Chem Res* **30**, 452–9 (1997).
5 Andreotti AH, Kahne D, Effects of glycosylation on peptide backbone conformation, *J Am Chem Soc* **115**, 3352–3 (1993).
6 Liang R, Andreotti AH, Kahne D, Sensitivity of glycopeptide conformation to carbohydrate chain length, *J Am Chem Soc* **117**, 10395–6 (1995).
7 Simanek EE, Huang D-H, Pasternack L, Machajewski TD, Seitz O, Millar DS, Dyson HJ, Wong C-H, Glycosylation of threonine of the repeating unit of RNA polymerase II with β-linked *N*-acetylglucosame leads to a turnlike structure, *J Am Chem Soc* **120**, 11567–75 (1998).
8 Mer G, Hietter H, Lefèvre J-F, Stabilization of proteins by glycosylation examined by NMR analysis of a fucosylated proteinase inhibitor, *Nat Struc Biol* **3**, 45–53 (1996).
9 Wyss DF, Choi JS, Li J, Knoppers MH, Willis KJ, Arulanandam ARN, Smolyar A, Reinhertz EL, Wagner G, Conformation and function of the *N*-linked glycan in the adhesion domain of human CD2, *Science* **269**, 1273–7 (1995).
10 Kihlberg J, Åhman J, Walse B, Drakenberg T, Nilsson A, Söderberg-Ahlm C, Bengtsson B, Olsson H, Glycosylated peptide hormones: Pharmacological proterties and conformational studies of analogues of [1-desamino,8-D-arginine]vasopressin, *J Med Chem* **38**, 161–9 (1995).
11 Kessler H, Matter H, Gemmecker G, Kottenhahn M, Bats JW, Structure and dynamics of a synthetic *O*-glycosylated cyclopeptide in solution determined by NMR spectroscopy and MD calculation, *J Am Chem Soc* **114**, 4805–18 (1992).
12 Otvos Jr H, Thurin J, Kollat E, Urge L, Mantsch HH, Hollosi M, Glycosylation of synthetic peptides breaks helices, *Int J Pept Protein Res* **38**, 476–82 (1991).
13 Hashimoto Y, Toma K, Nishikido J, Yamamoto K, Haneda K, Inazu T, Valentine KG, Opella SJ, Effects of glycosylation on the structure and dynamics of eel calcitonin in micelles and lipid bilayers determined by nuclear magnetic resonance spectroscopy, *Biochemistry* **38**, 8377–84 (1999).
14 Tagashira M, Tanaka A, Hisatani K, Isogai Y, Hori M, Takamatsu S, Fujibayashi Y, Yamamoto K, Haneda K, Inazu T, Toma K, Effect of carbohydrate structure on biological activity of artificially *N*-glycosylated eel calcitonin, *Glycoconjugate J* **18**, 449–55 (2001).
15 Tagashira M, Iijima H, Isogai Y, Hori M, Takamatsu S, Fujibayashi Y, Haneda K, Inazu T, Toma K, Site-independent activity enhancement of calcitonin by *N*-acetylglucosamine attachment. In *Peptide Science 2000*, edited by Shioiri T (The Japanese Peptide Society, Osaka, 2001) pp. 125–8.
16 Tagashira M, Iijima H, Isogai Y, Hori M, Takamatsu S, Fujibayashi Y, Kumagaye KY, Isaka S, Nakajima K, Yamamoto T, Teshima T, Toma K, Site-dependent effect of *O*-glycosylation on the conformation and biological activity of calcitonin, *Biochemistry* **40**, 11090–5 (2001).
17 Tagashira M, Iijima H, Toma K, Three-dimensional structure and biological activity of glycosylated calcitonin, *Trends Glycosci Glycotechnol* **13**, 373–83 (2001).
18 Azria M, *The Calcitonins: Physiology and Pharmacology* (Karger, Basel, Switzerland, 1989).
19 Motta A, Morelli MAC, Goud N, Temussi PA, Sequencial ^{1}H-NMR assignment and secondary structure determination of salmon calcitonin in solution, *Biochemistry* **28**, 7996–8002 (1989).
20 Meadows RP, Nikonowicz EP, Jones CR, Bastian JW, Gorenstein DG, Two-dimensional NMR and structure determination of salmon calcitonin in methanol, *Biochemistry* **30**, 1247–54 (1991).
21 Epand RM, Epand RF, Orlowski RC, Schlueter RJ, Boni LT, Hui SW, Amphipathic helix and its relationship to the interaction of calcitonin with phospholipids, *Biochemistry* **22**, 5074–84 (1983).
22 Lin HY, Harris TL, Flannery MS, Aruffo A, Kaji EH, Gorn A, Kolakowski LF, Lodish HF, Goldring SR, Expression cloning of an adenylate cyclase-coupled calcitonin receptor, *Science* **254**, 1022–6 (1991).
23 Wüthrich K, *NMR of Proteins and Nucleic Acids* (J. Wiley & Sons, New York, 1986).
24 Ogawa K, Nishimura S, Uchiyama S, Kobayashi K, Kyogoku Y, Hayashi M, Kobayashi Y, Conformation analysis of eel calcitonin—comparison with the conformation of elcatonin, *Eur J Biochem* **257**, 331–6 (1998).

25 Dalgarno DC, Levine BA, Williams RJP, Structural information from NMR secondary chemical shifts of peptide αC-H protons in proteins, *Biosci Rep* **3**, 443–52 (1983).
26 Sternlicht H, Wilson D, Magnetic resonance studies of macromolecules. I. Aromatic-methyl interactions and helical structure effects in lysozyme, *Biochemistry* **6**, 2881–92 (1967).
27 Epand RM, Epand RE, Stafford AR, Orlowski RC, Deletion sequences of salmon calcitonin that retain the essential biological and conformational features of the intact molecule, *J Med Chem* **31**, 1595–8 (1988).

Received 27 June 2002; revised 23 September 2002;
accepted 14 November 2002